COST Action IC 1407 – Training School
Malta, April 19-20, 2018

REVERBERATION CHAMBERS

V. Mariani Primiani
Università Politecnica delle Marche
Dept. Information Engineering
60131 Ancona - Italy

COST is supported by
the EU Framework Programme
Horizon 2020

COST Association
Avenue Louise 149 I 1050 Brussels, Belgium
t: +32 (0)2 533 3800 I f: +32 (0)2 533 3890
office@cost.eu I www.cost.eu

Definition of Reverberation Chamber

A properly operating RC is an electrically large cavity, where the electromagnetic field is statistically uniform, isotropic and randomly polarised within an acceptable and predictable uncertainty and confidence limit

- Uniformity implies all spatial locations within RC (at sufficient distance from metal surfaces) are equivalent
- Isotropic implies that at given location in RC electromagnetic energy is same in any direction
- Random polarization implies that the phase relationships between polarized components are equivalent

…….electrically large cavity…

Time Domain

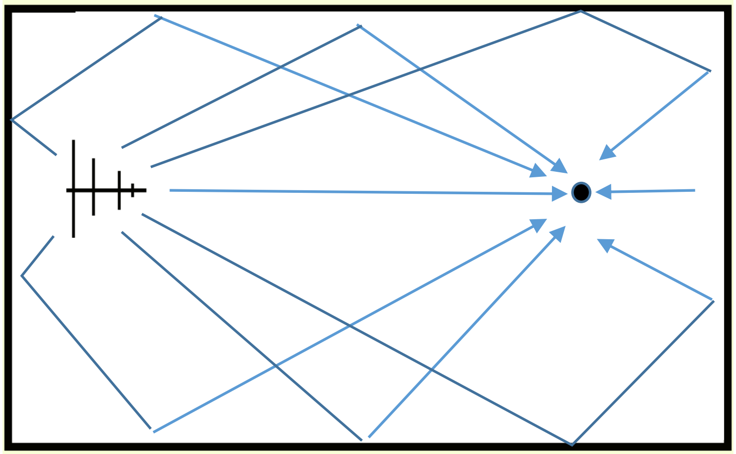

$$\vec{e}_T = \sum_{n=1}^{\infty} \vec{e}_n(t-\tau_n)\,u(t-\tau_n)$$

$$u(t-\tau_n) = \begin{cases} 1 \; if \; t \geq \tau_n \\ 0 \; if \; t < \tau_n \end{cases}$$

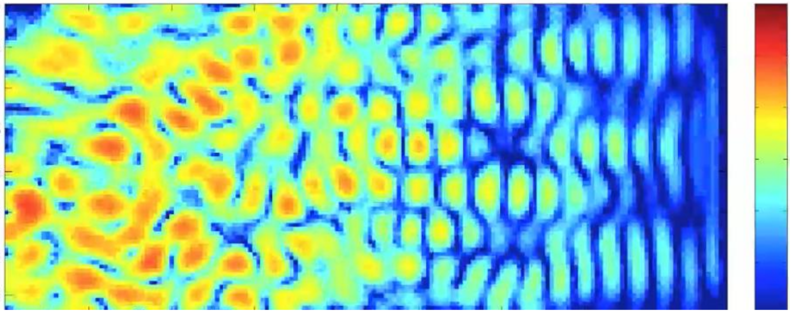

…….electrically large cavity…

Frequency Domain

$$\vec{E} = -\frac{1}{j\omega\varepsilon}\sum_{m=0}^{\infty}\sum_{n=0}^{\infty}\sum_{p=0}^{\infty}\frac{\int_V \vec{J}\cdot\vec{f}_{mnp}\,dV}{\int_V \left|\vec{f}_{mnp}\right|^2 dV}\vec{f}_{mnp} - j\omega\mu\sum_{m=0}^{\infty}\sum_{n=0}^{\infty}\sum_{p=0}^{\infty}\frac{\int_V \vec{J}\cdot\vec{e}_{mnp}\,dV}{\left(k_{mnp}^2-\tilde{k}^2\right)\int_V \left|\vec{e}_{mnp}\right|^2 dV}\vec{e}_{mnp}$$

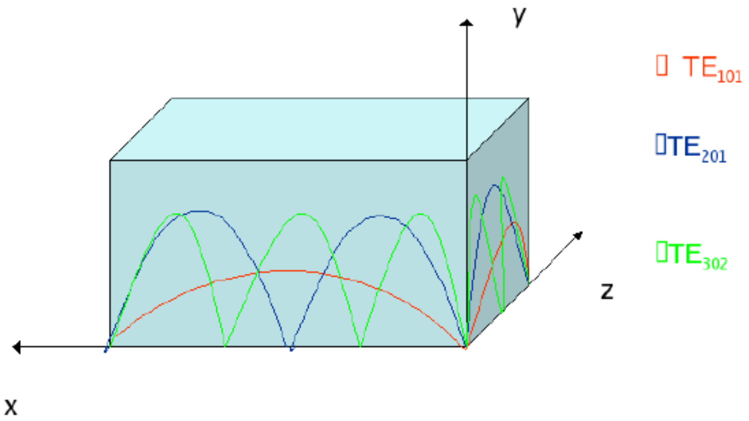

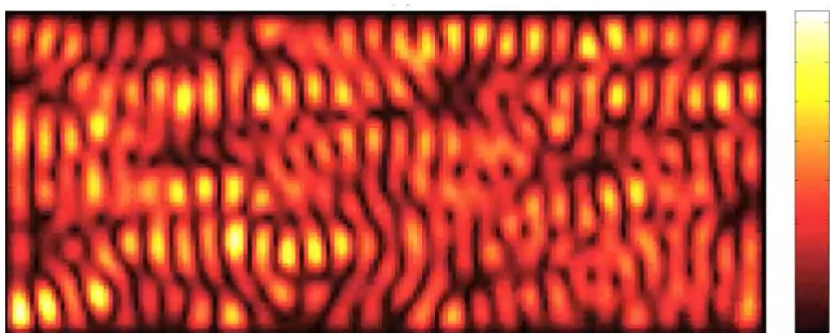

Cavity modes

$$f_{mnp} = \frac{c}{2}\sqrt{\left(\frac{m}{a}\right)^2 + \left(\frac{n}{b}\right)^2 + \left(\frac{p}{d}\right)^2}$$

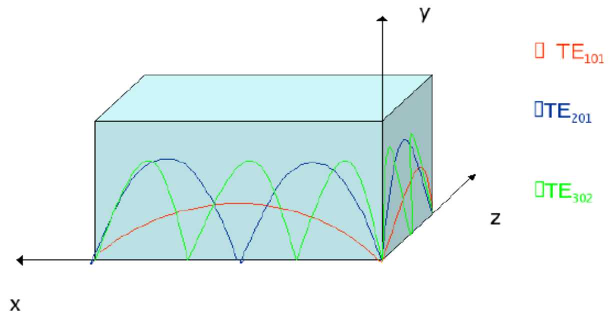

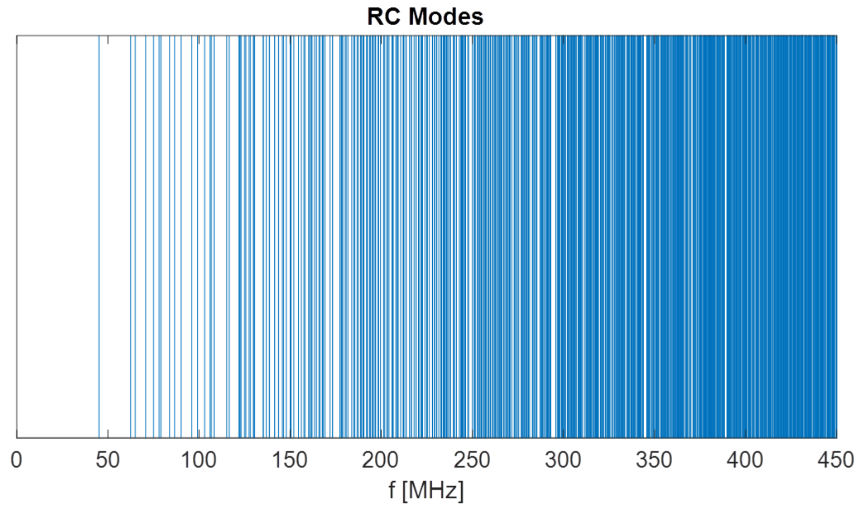

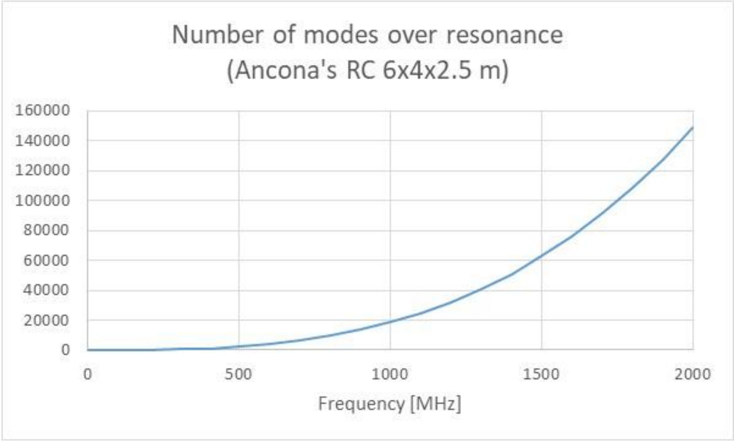

$$N = \frac{8\pi}{3} V \left(\frac{f}{c}\right)^3 - (a+b+d)\left(\frac{f}{c}\right) + \frac{1}{2}$$

Cavity modes

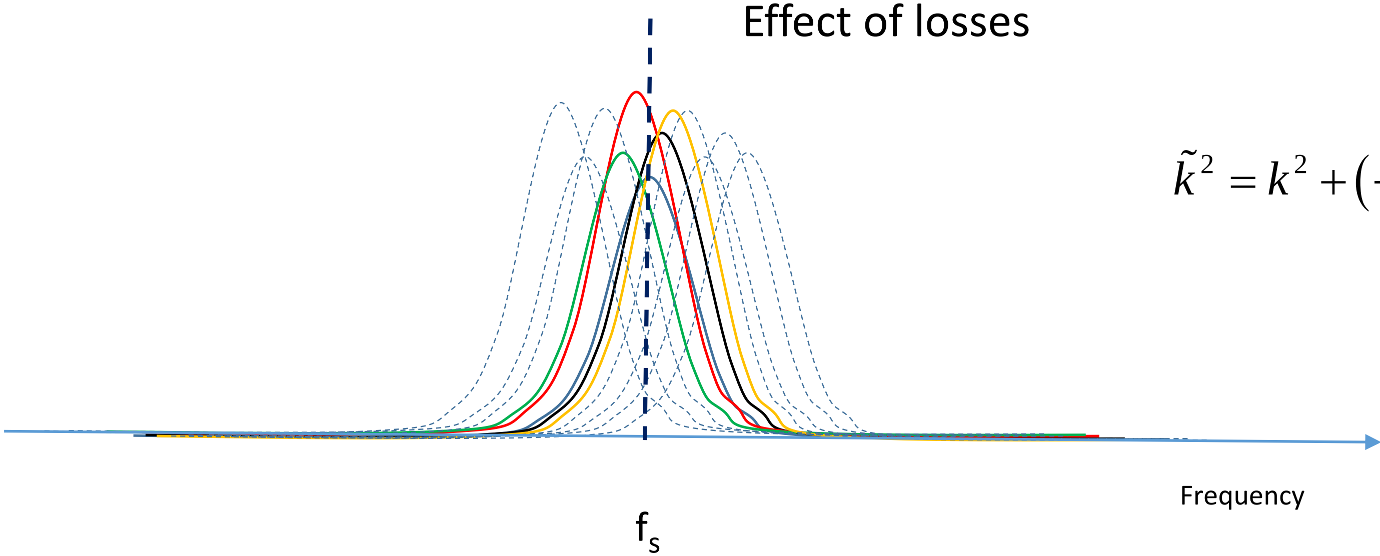

$$\tilde{k}^2 = k^2 + (-1 + j)\frac{k^2 \omega_m}{Q_m \omega}$$

$$\frac{dN}{df} = \frac{8\pi V}{c^3} f^2$$

$$BW \approx f / Q$$

$$N_S = \frac{8\pi V f^3}{c^3 Q}$$

Rule of thumb: at least 60 modes over resonance (typically it happens between 3 F_o and 6 F_o)

……statistically uniform, isotropic and randomly polarised

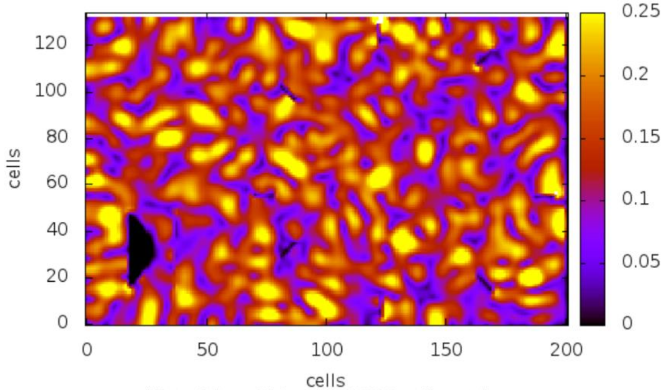

For TE_{mnp} $E_z=0$

For TM_{mnp} $H_z=0$

For a single chamber state

- No uniformity
- No isotropy
- No random polarization

$$\vec{E} = \ldots - j\omega\mu \sum_{m=0}^{\infty}\sum_{n=0}^{\infty}\sum_{p=0}^{\infty} \frac{\int_V \vec{J}\cdot\vec{e}_{mnp}\, dV}{\left(k_{mnp}^2-\tilde{k}^2\right)\int_V \left|\vec{e}_{mnp}\right|^2 dV}\,\vec{e}_{mnp}$$

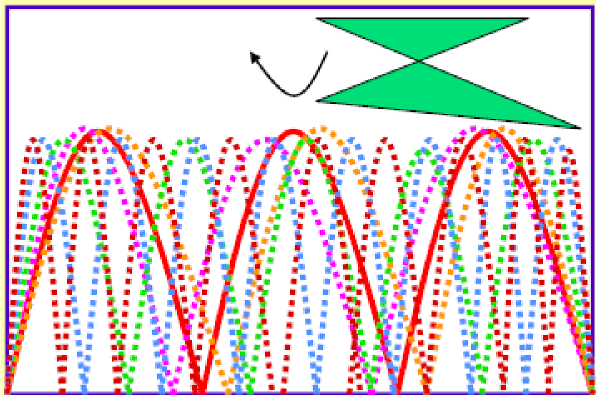

We need a stirring action to get a lot of different chamber realizations

Example of mechanical stirring

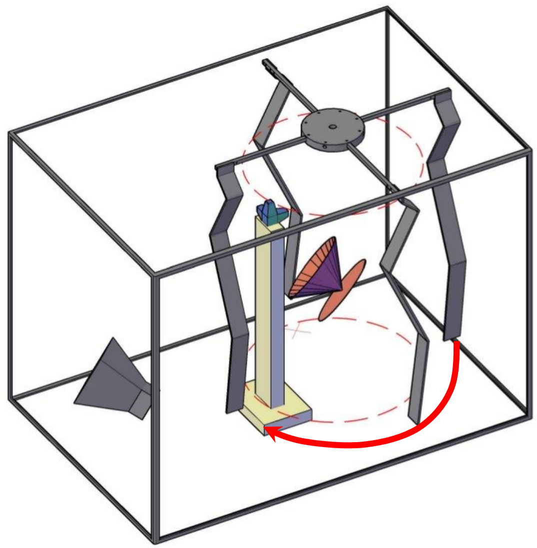

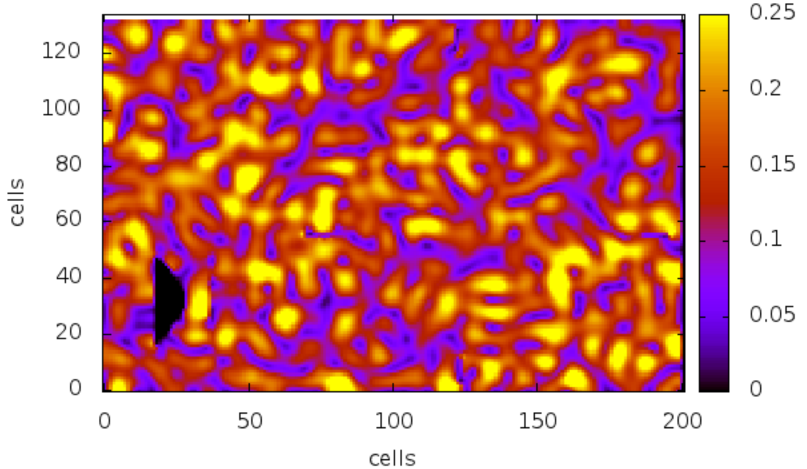

F. Moglie and V. Mariani Primiani, "Numerical Analysis of a New Location for the Working Volume Inside a Reverberation Chamber," in *IEEE Transactions on Electromagnetic Compatibility*, vol. 54, no. 2, pp. 238-245, April 2012.

Sample #	Prec.	Ex	Ey	Ez
1				
2				
3				
4				
5				
.....				
.....				
.....				
N				

Ensemble average , mean value ($<X>_N$)
Maximum value
Max/Mean ratio
Statistical distributions: PDF and CDF.

Field stirring actions

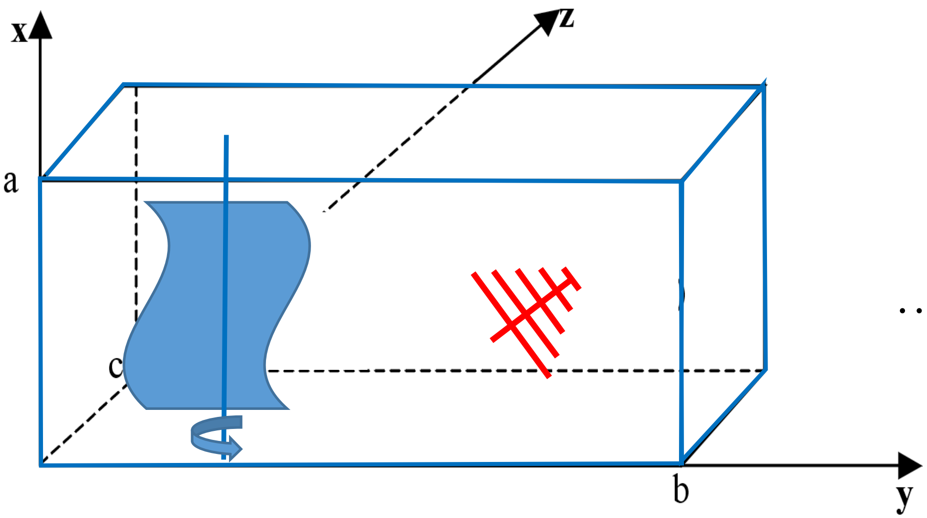

Source stir. Mechanical

$$\cdots j\omega\mu \sum_{m=0}^{\infty}\sum_{n=0}^{\infty}\sum_{p=0}^{\infty} \frac{\int_V \vec{J}\cdot\vec{e}_{mnp}\,dV}{\left(k_{mnp}^2-\tilde{k}^2\right)\int_V \left|\vec{e}_{mnp}\right|^2 dV}\,\vec{e}_{mnp}$$

MECHANICAL STIRRING, i.e. boundary condition variations

- ❑ Rotating paddles (NIST group, …..)
- ❑ Moving walls (Capsalis, …)
- ❑ Vibrating walls (VIRC by Leferink, ..)
- ❑ ………….

SOURCE STIRRING

- ❑ Generator amplitude or phase variation (Hill, …)
- ❑ Frequency variation (frequency stirring) (T. A. Loughry, …)
- ❑ Moving transmitting antenna to change mode coupling (Huang, Carlberg, Kildal, …)
- ❑ ….

For a review and history of all techniques see R. Serra, A. Marvin, F. Leferink, V. Mariani Primiani, F. Moglie, M. O. Hatfield, Y. Huang. L. Arnaut, A. Cozza. M. Klinger, "Reverberation chambers a la carte: An overview of the different mode-stirring techniques," in *IEEE Electromagnetic Compatibility Magazine*, vol. 6, no. 1, pp. 63-78, First Quarter 2017.

Statistical distributions in an ideal RC

$$E_x = E_{xr} + iE_{xi}, \quad E_y = E_{yr} + iE_{yi}, \quad E_z = E_{zr} + iE_{zi}$$

$$< E_{xr} > = < E_{xi} > = < E_{yr} > = < E_{yi} > = < E_{zr} > = < E_{zi} > = 0$$

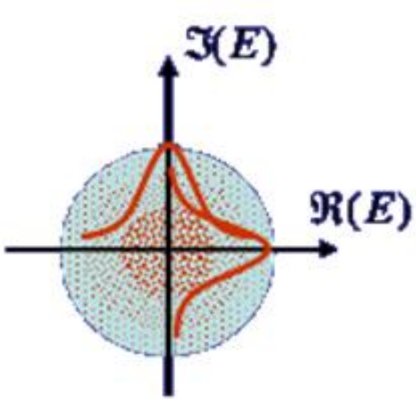

$$f(E_{xr}) = \frac{1}{\sqrt{2\pi}\sigma} \exp\left[-\frac{E_{xr}^2}{2\sigma^2} \right]$$

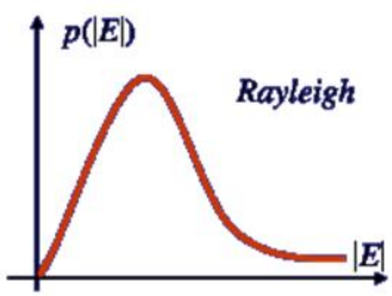

CHI-2DOF (χ_2)

$$f(| E_x |) = \frac{| E_x |}{\sigma^2} \exp\left[-\frac{| E_x |^2}{2\sigma^2} \right]$$

Distribution of the received power P_R or of $\left|E_i\right|^2$

CHI²-2DOF $\qquad \chi_2^2 \qquad$ $$f(|E_x|^2) = \frac{1}{2\sigma^2}\exp\left[-\frac{|E_x|^2}{2\sigma^2}\right]$$

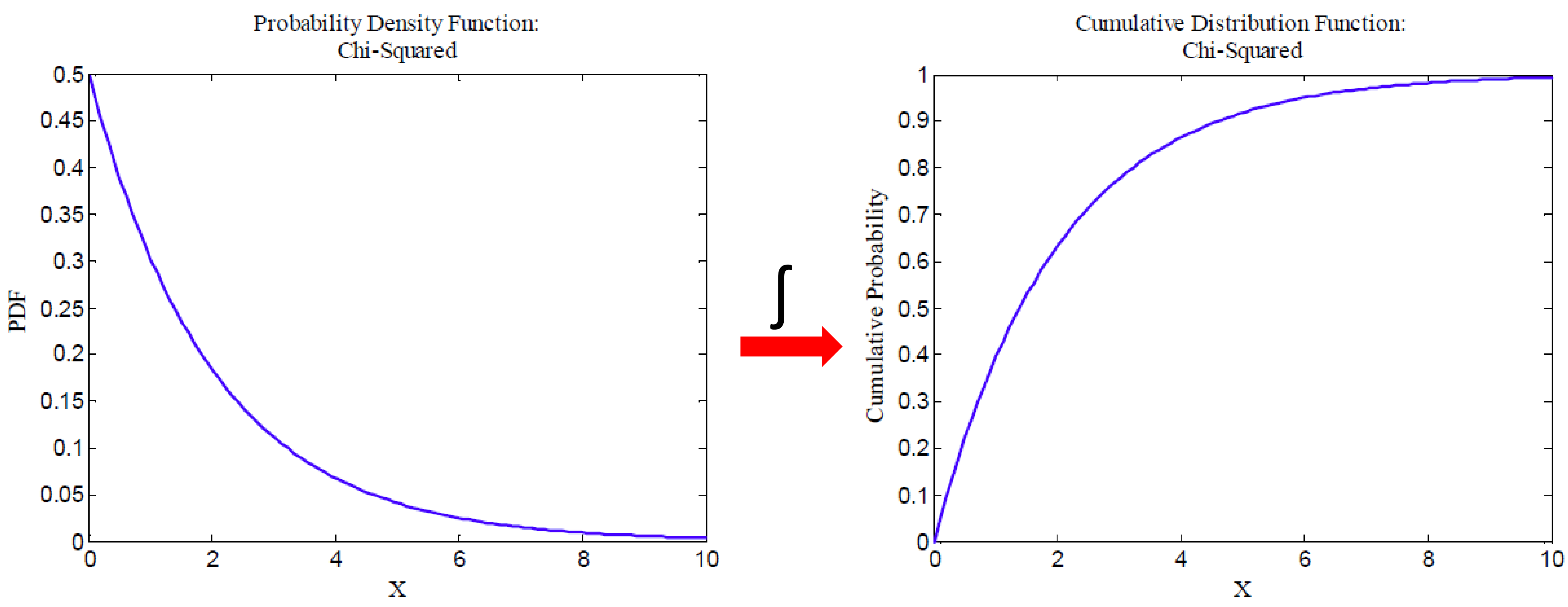

Statistical distribution of the total E-field

CHI-6DOF χ_6

$$f(|E|) = \frac{|E|^5}{8\sigma^6} \exp\left[-\frac{|E|^2}{2\sigma^2}\right]$$

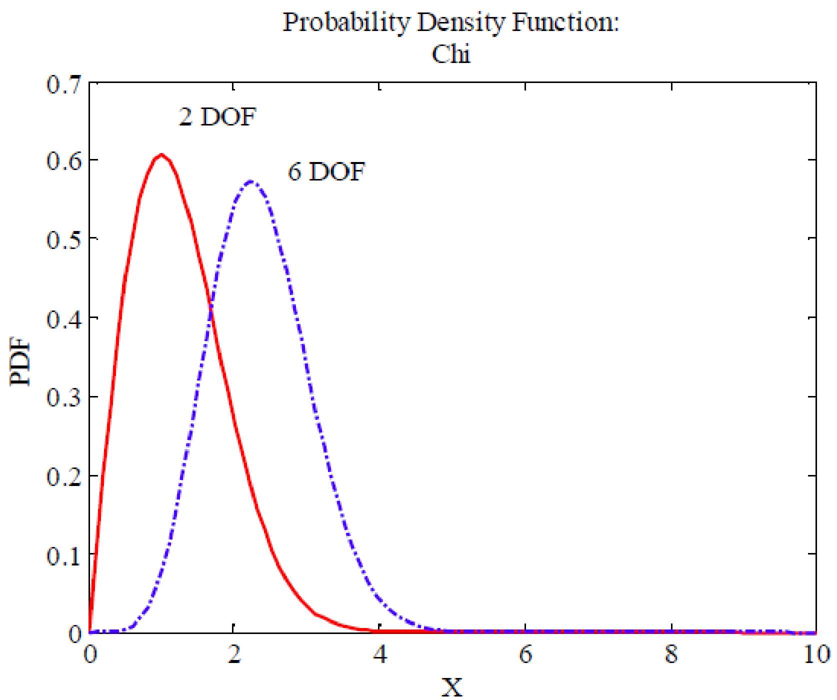

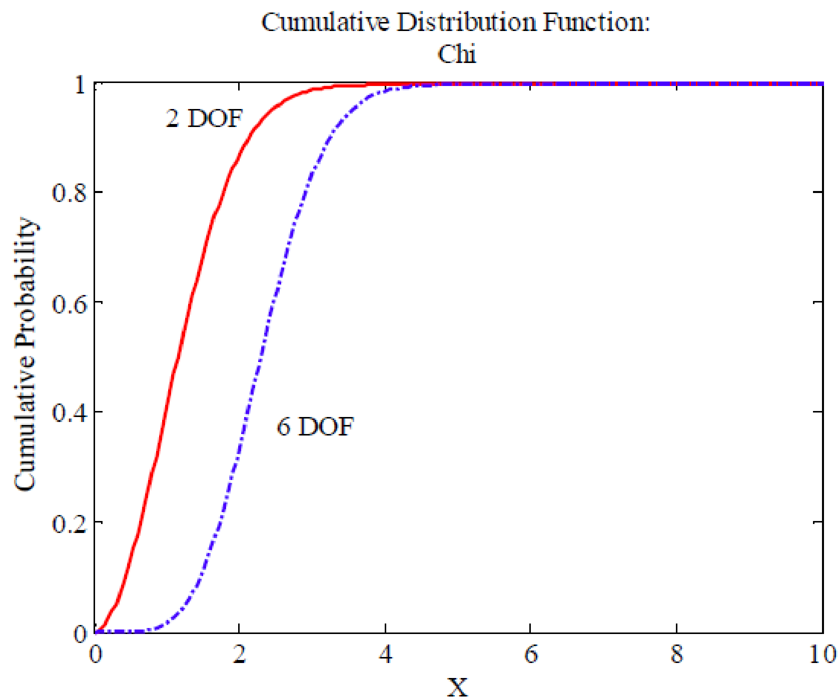

An elegant view of the ideal RC field: the plane wave integral representation (by Hill)

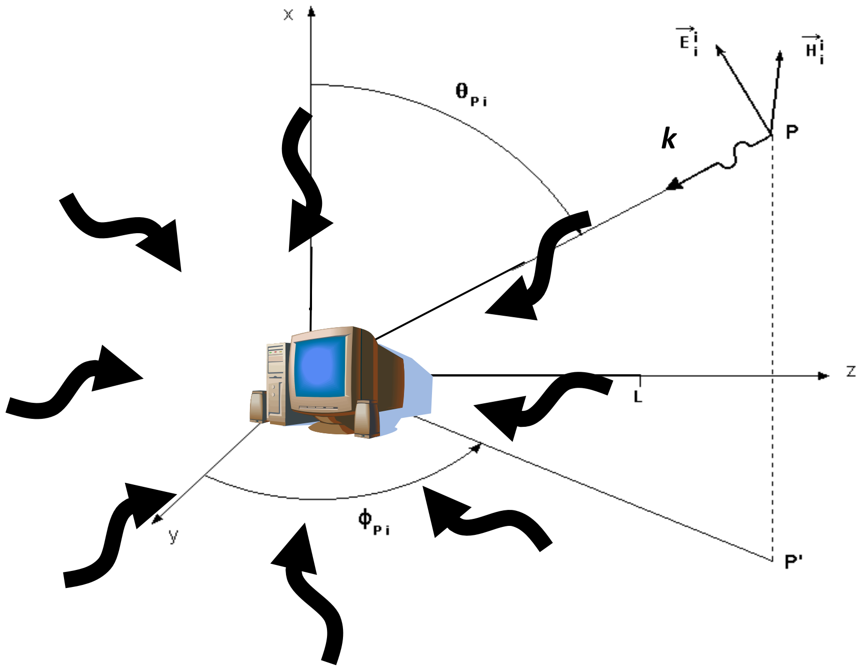

$$E(r) = \iint_{4\pi} F(\Omega)\exp(ik \bullet r)\,d\Omega,$$

$$k = -k(\hat{x}\sin\alpha\cos\beta + \hat{y}\sin\alpha\sin\beta + \hat{z}\cos\alpha).$$

$$< E(r) > = \iint_{4\pi} < F(\Omega) > \exp(ik \bullet r)\,d\Omega = 0$$

$$|E(r)|^2 = \iint_{4\pi}\iint_{4\pi} F(\Omega_1) \bullet F^*(\Omega_2)\exp[i(k_1 - k_2) \bullet r]\,d\Omega_1\,d\Omega_2 \equiv E_0^2$$

$$S = \frac{E_0^{\;2}}{377}$$

Scalar Power Density

Antenna behaviour in ideal RC

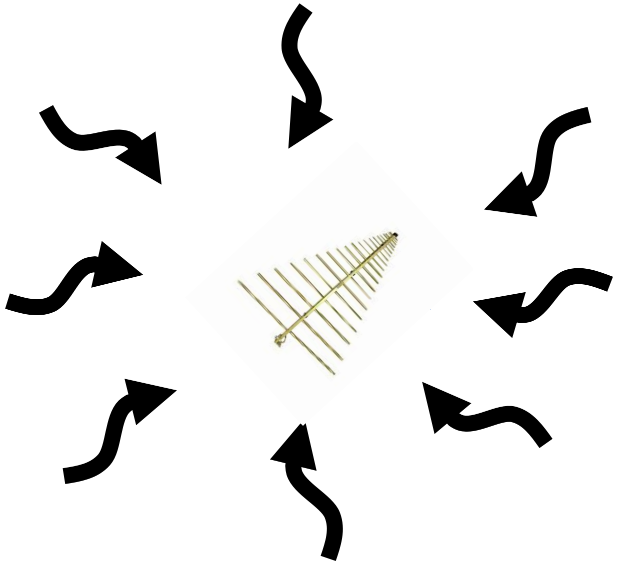

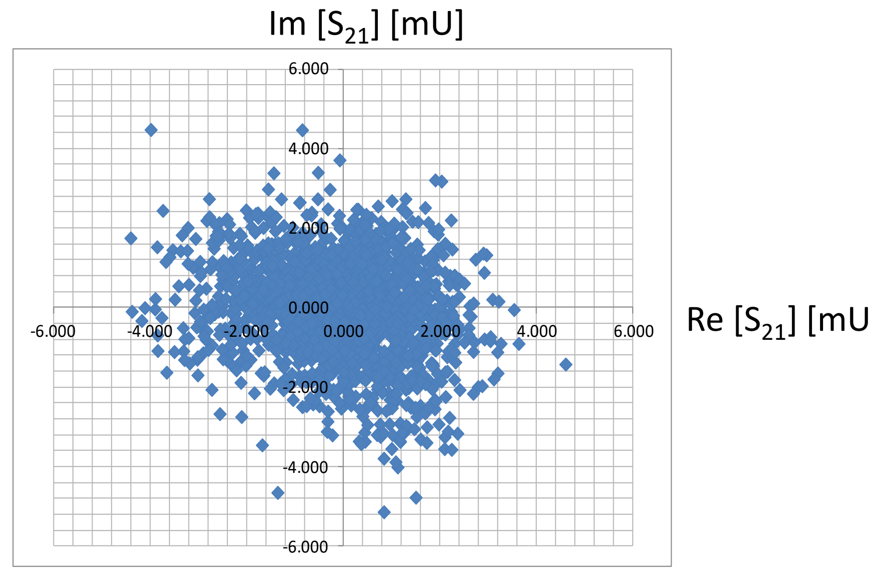

$$\langle D \rangle = \langle g_D(\theta,\varphi) \rangle = 1$$

$$\langle A_{eff} \rangle = \frac{1}{2} \frac{\lambda^2}{4\pi}$$

Free space A_{eff}/D

Polarization mismatching

$$\langle P_R \rangle = S \cdot \langle A_{eff} \rangle \cdot m \cdot \eta_{RX} = S \cdot \frac{\lambda^2}{8\pi} \cdot m \cdot \eta_{RX}$$

$$m = \langle (1 - |S_{11}|^2) \rangle \simeq (1 - |\langle S_{11} \rangle|^2)$$

η_{RX} Antenna efficiency (effect of antenna losses)

Example of received power statistics

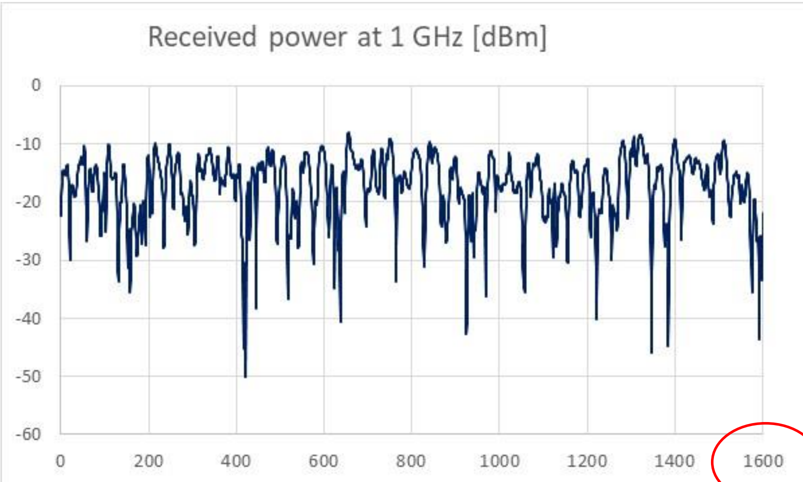

Chamber dimensions 6 x4 x2.5 m

Stirring ratio 42 dB

Number of independent samples N_{ind} = 200

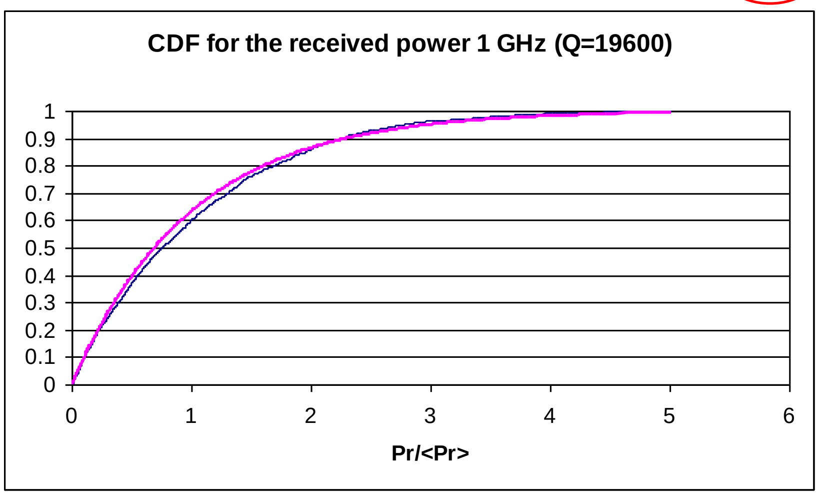

$$CDF\left\{\chi_2^2(s)\right\} = 1 - \exp\{-s\}$$

s = mean normalised received power

Theor.

Exp.

Determination of uncorrelated stirrer positions

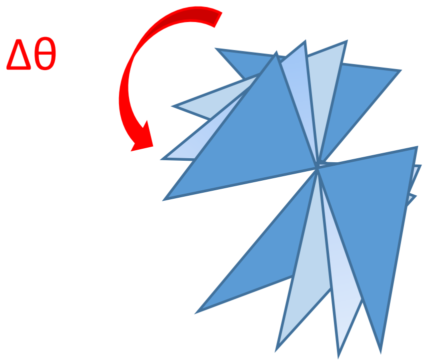

$$r = \frac{\frac{1}{n-1}\sum_{i}^{n}(x_i - u_x)(y_i - u_y)}{\sqrt{\left(\frac{\sum_{i}^{n}(x_i - u_x)^2}{n-1}\right)\left(\frac{\sum_{i}^{n}(y_i - u_y)^2}{n-1}\right)}}$$

$$r \approx 0.37 \cdot \left(1 - \frac{7.22}{n^{0.64}}\right)$$

Circular autocorrelation

1601 values

											M = 1601/8	200
	0.968247	0.885106	0.774307	0.656979	0.546131	0.447477	0.362268	0.289546	0.22754	0.1746		
	shift 1	shift 2	shift 3	shift 4	shift 5	shift 6	shift 7	shift 8	shift 9	shift 10		
0.07587	0.079966	0.048021	0.024816	0.021428	0.036721	0.049407	0.051975	0.043173	0.024282	0.006603		
0.11349	0.07587	0.079966	0.048021	0.024816	0.021428	0.036721	0.049407	0.051975	0.043173	0.024282		
0.144328	0.11349	0.07587	0.079966	0.048021	0.024816	0.021428	0.036721	0.049407	0.051975	0.043173		
0.169102	0.144328	0.11349	0.07587	0.079966	0.048021	0.024816	0.021428	0.036721	0.049407	0.051975		
0.18441	0.169102	0.144328	0.11349	0.07587	0.079966	0.048021	0.024816	0.021428	0.036721	0.049407		
0.18675	0.18441	0.169102	0.144328	0.11349	0.07587	0.079966	0.048021	0.024816	0.021428	0.036721		
"	"	"	"	"	"	"	"	"	"	"		
"	"	"	"	"	"	"	"	"	"	"		
"	"	"	"	"	"	"	"	"	"	"		
"	"	"	"	"	"	"	"	"	"	"		
"	"	"	"	"	"	"	"	"	"	"		
0.049407	0.051975	0.043173	0.024282	0.006603	0.029461	0.046321	0.049953	0.047316	0.046356	0.054704		
0.036721	0.049407	0.051975	0.043173	0.024282	0.006603	0.029461	0.046321	0.049953	0.047316	0.046356		
0.021428	0.036721	0.049407	0.051975	0.043173	0.024282	0.006603	0.029461	0.046321	0.049953	0.047316		
0.024816	0.021428	0.036721	0.049407	0.051975	0.043173	0.024282	0.006603	0.029461	0.046321	0.049953		
0.048021	0.024816	0.021428	0.036721	0.049407	0.051975	0.043173	0.024282	0.006603	0.029461	0.046321		
0.079966	0.048021	0.024816	0.021428	0.036721	0.049407	0.051975	0.043173	0.024282	0.006603	0.029461		

Stirrer independent (uncorrelated) positions

…….within an acceptable and predictable uncertainty and confidence limit.

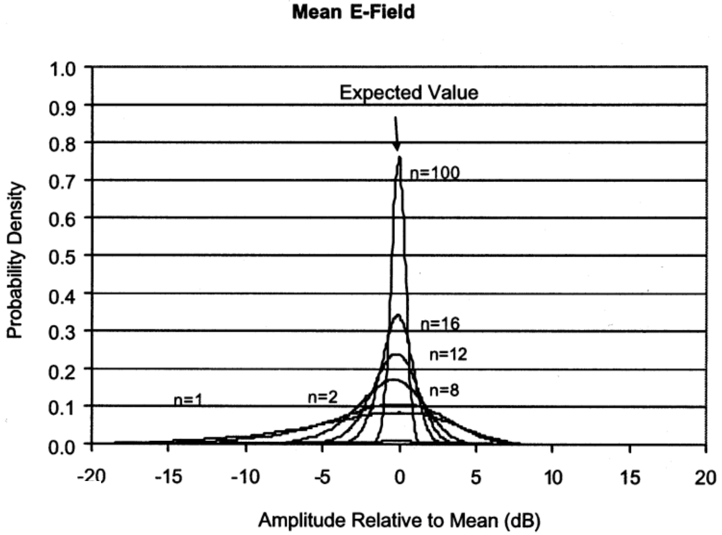

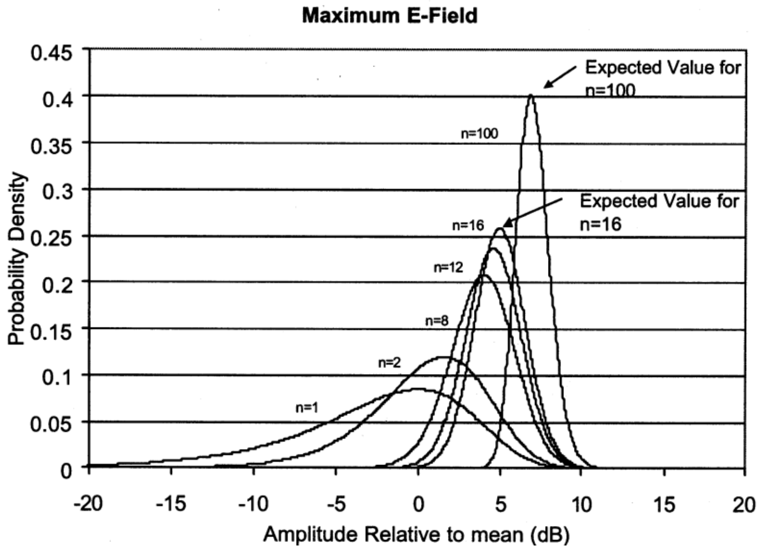

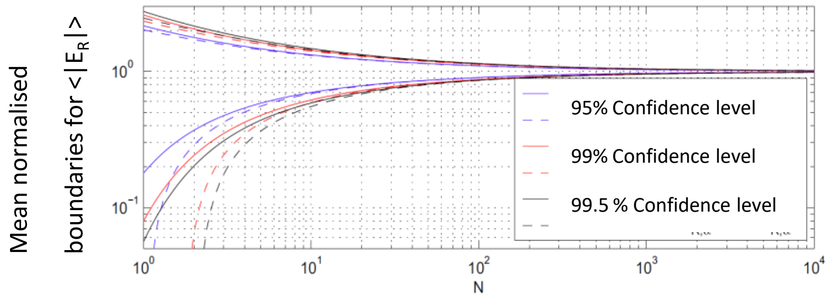

$$PDF(r) = M\frac{\pi}{2}r\left[1-e^{\left(-\frac{\pi}{4}r^2\right)}\right]^{M-1}e^{\left(-\frac{\pi}{4}r^2\right)} \qquad r=\frac{E_{\max}}{\langle E\rangle}$$

See Appendix K of IEC 61000-4-21 and related references for uncertainty as function of N and confidence level

Chamber quality factor

$$Q = \frac{\omega U}{P_D} = \frac{1}{\frac{1}{Q_w} + \frac{1}{Q_{Ant}} + \frac{1}{Q_{Abs}} + \frac{1}{Q_{Other}}}$$

$$Q_w \approx \frac{3V}{2\mu_r \delta A} \propto \sqrt{f} \qquad \delta = 1/\sqrt{\pi f \sigma \mu}$$

$$Q_{Ant} = \frac{16\pi^2 V}{m\lambda^3} \propto f^3$$

$$Q_{Abs} = \frac{2\pi V}{\lambda \langle \sigma_a \rangle_\Omega} \propto f$$

Measured Q $\quad Q = \frac{16\pi^2 V}{\eta_{Tx}\eta_{Rx}\lambda^3}\left\langle \frac{P_{AveRec}}{P_{Input}} \right\rangle_n$

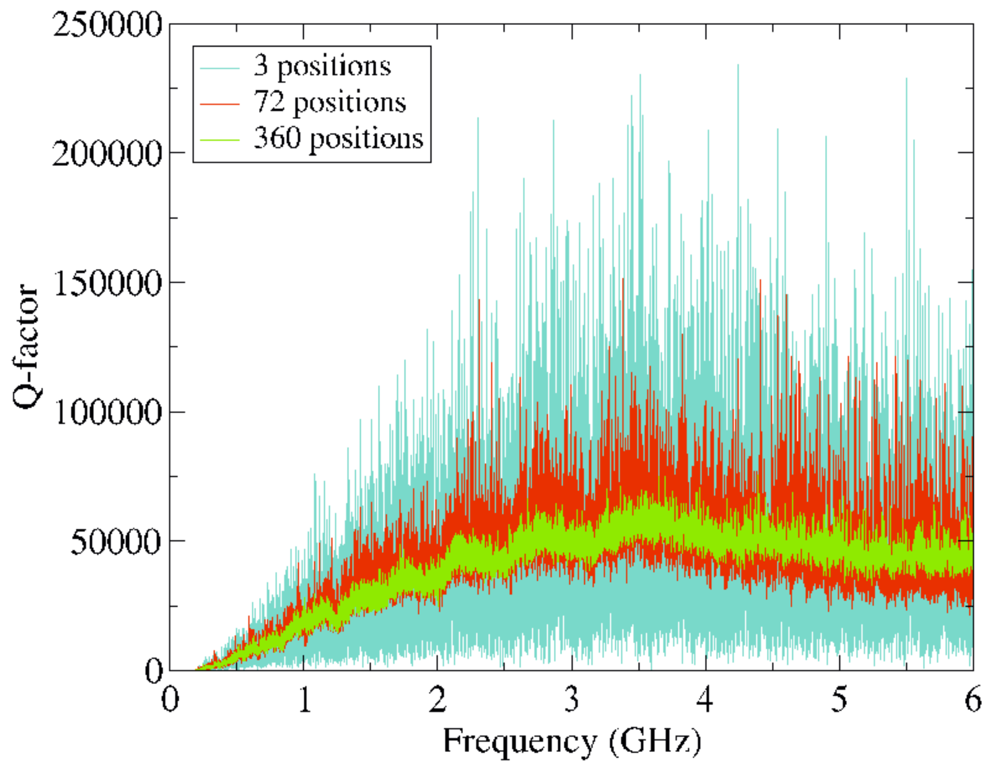

Another chamber performance indicator: the field uniformity

$$\overleftrightarrow{E}_{x,y,z} = \frac{E_{MAX\ x,y,z}}{\sqrt{P_{INPUT}}} ,$$

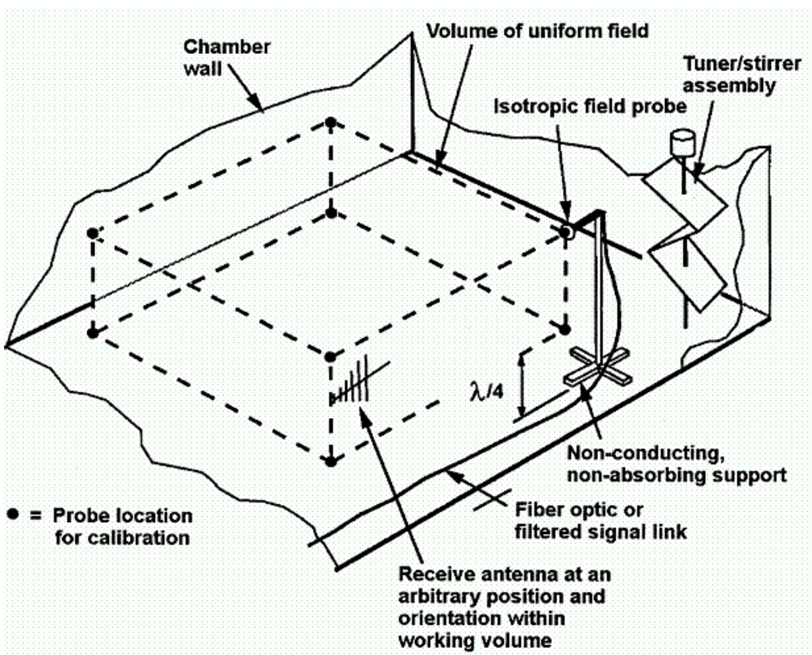

$$\left\langle \overleftrightarrow{E}_x \right\rangle_8 = \left(\sum \overleftrightarrow{E}_x \right) \Big/ 8$$

$$\left\langle \overleftrightarrow{E}_y \right\rangle_8 = \left(\sum \overleftrightarrow{E}_y \right) \Big/ 8$$

$$\left\langle \overleftrightarrow{E}_z \right\rangle_8 = \left(\sum \overleftrightarrow{E}_z \right) \Big/ 8$$

$$\left\langle \overleftrightarrow{E} \right\rangle_{24} = \left(\sum \overleftrightarrow{E}_{x,y,z} \right) \Big/ 24,$$

Field uniformity in the working volume

$$\sigma_x = \sqrt{\frac{\sum\left(E_{ix} - \langle E_x \rangle_8\right)^2}{8-1}}$$

$$\sigma_{24} = \sqrt{\frac{\sum_{m=1}^{8} \sum_{n=1}^{3}\left(E_{m,n} - \langle E \rangle_{24}\right)^2}{24-1}}$$

$$\sigma(db) = 20 \cdot \log\left(\frac{\sigma + \langle E_{xyz} \rangle}{\langle E_{xyz} \rangle}\right)$$

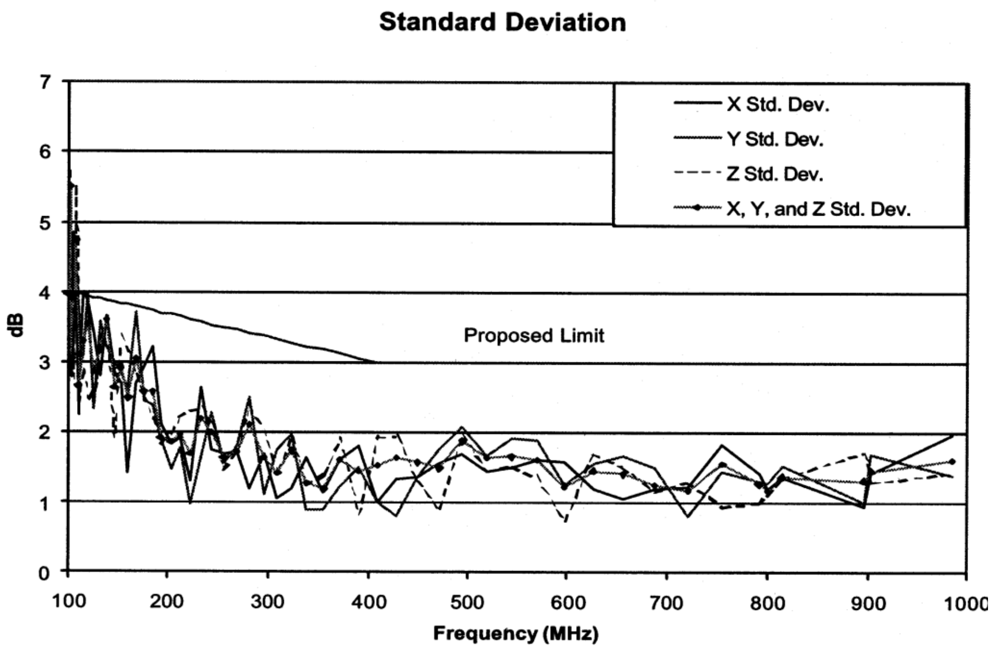

IEC 61000-4-21

Improvements of Chamber performance

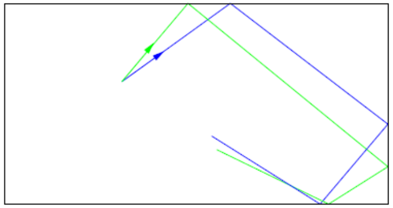

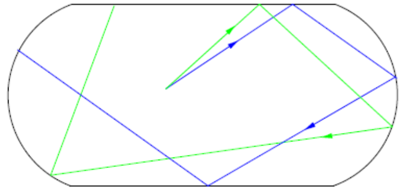

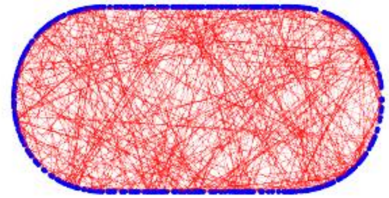

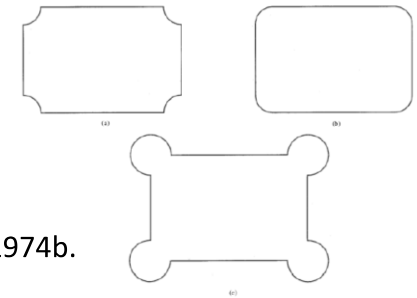

L.A. Bunimovich, “The ergodic properties of certain billiards”, Funkt. Anal.Prilozh. 8:73-74,1974b.
H.J. Stockmann, “Quantum Chaos”: An Introduction”, Cambridge University Press, 2006.

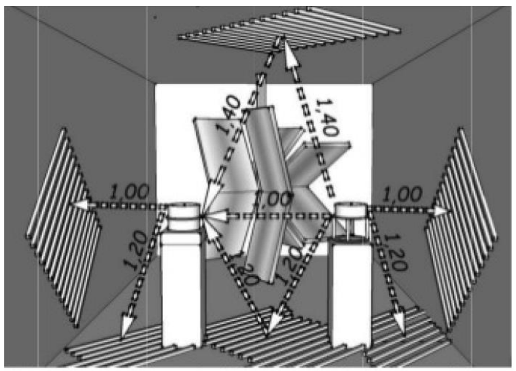

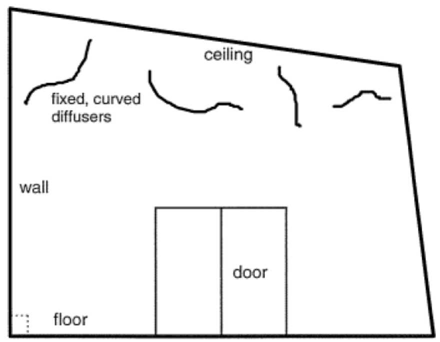

F. Leferink, “High Field Strength in a Large Volume: The Intrinsic Reverberation Chamber”, IEEE EMC 1998, Denver, CO, USA

L. Arnaut, “Operation of electromagnetic reverberation chambers with wave diffractors at relatively low frequencies”, IEEE Trans. on EMC 2001, pp. 637-653, Vol. 43, No. 4, Nov.

A. C. Marvin, E. Karadimou, ”The Use of Wave Diffusers to Reduce the Contribution of Specular Wall Reflections to the Unstirred Energy in a Reverberation Chamber”, IEEE EMC 2013, Denver, CO, USA

K. Selemani, J.-B. Gros, E. Richalot, O. Legrand, O. Picon and F. Mortessagne, “Comparison of reverberation chamber shapes inspired from chaotic cavities”, IEEE Trans. on EMC 2015, pp. 3-11, Vol. 57, No. 1, Feb

Typical RC applications

IEC 61000-4-21
Electromagnetic compatibility (**EMC**) - Part 4-21: Testing and measurement techniques – Reverberation chamber test methods

- **Emission measurements**
- **Immunity tests**
- **Shielding effectiveness of**
  - **Enclosures**
  - **Cables**
  - **Gaskets**
  - **Materials**
- **Antenna efficiency**

Others

- **Material characterizations in terms of:**
  - **Absorbing cross section**
  - **Scattering cross section**
- **Testing of wireless devices and systems**
  - **Multipath propagation**
  - **Transmission quality**
- **……………………………….**

Emission tests

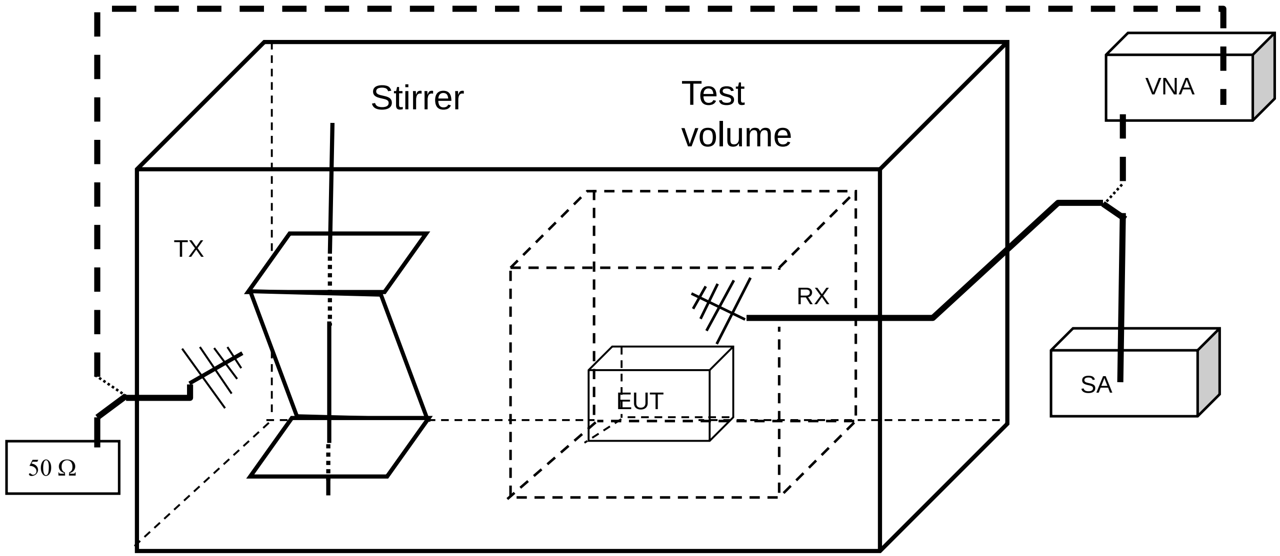

$$P_{RAD} = \frac{<P_r> 16\pi^2 V}{\eta_{TX}\eta_{RX}\lambda^3 Q}$$

Follow the procedure in Annex B of IEC standard to account for Q variations with the EUT

Correlation with traditional methods

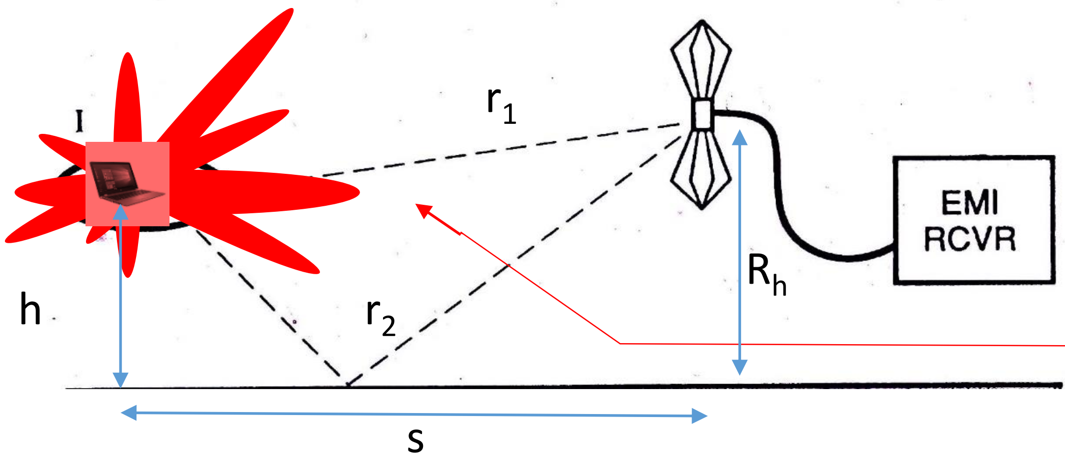

$$E_{\max} = g_{\max}\sqrt{\frac{DP_{RAD}377}{4\pi R^2}}$$

D_{MAX} = ?

$$g_{\max} = \begin{cases} \left| \frac{r}{r_1} e^{-jkr_1} - \frac{r}{r_2} e^{-jkr_2} \right|_{\max} & \text{for horizontal polarization} \\ \left| \frac{s^2}{r_1^2} \frac{r}{r_1} e^{-jkr_1} + \frac{s^2}{r_2^2} \frac{r}{r_2} e^{-jkr_2} \right|_{\max} & \text{for vertical polarization} \end{cases}$$

$$r = \sqrt{s^2 + R_h^2}$$

Typically for s = 10 m and $1 \leq R_h \geq 4$m, $g_{max} \approx 2$

Example

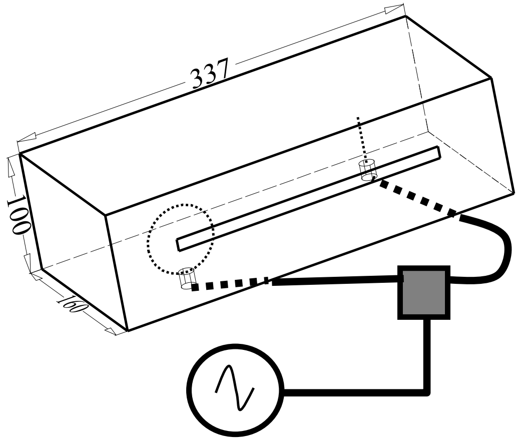

Aperture dimensions:

228 x 2.5 mm

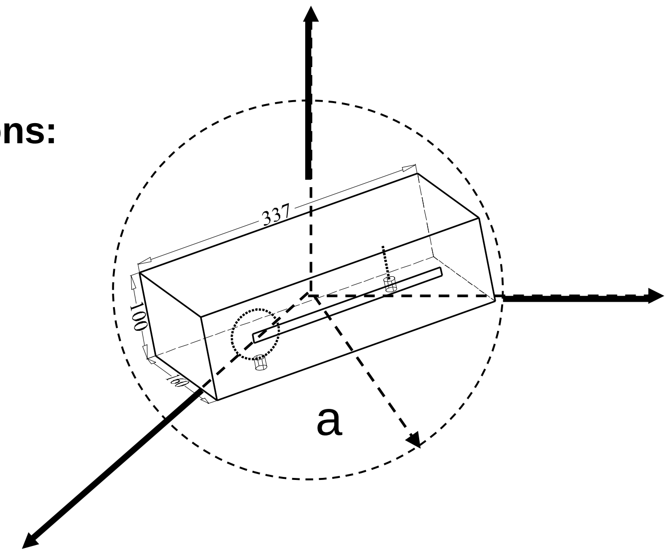

$$D = \begin{cases} 1{,}55 & \text{per } ka \le 1 \\ 0{,}5\left(0{,}577 + \ln\left(4(ka)^2 + 8ka\right) + \dfrac{1}{8(ka)^2 + 16ka}\right) & \text{per } ka > 1 \end{cases}$$

MHz	500	550	600	650	700	750	800	850	900	950	1000	1050	1100
D	2,89	2,97	3,04	3,11	3,17	3,23	3,28	3,33	3,38	3,43	3,48	3,52	3,56

Results

Total radiated power

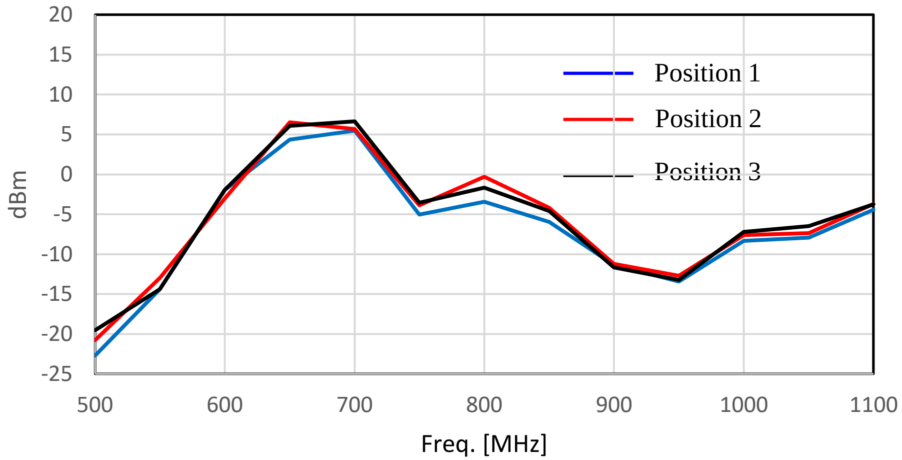

Independence on EUT positioning (within the acceptable uniformity)

Electric field: RC vs. OATS

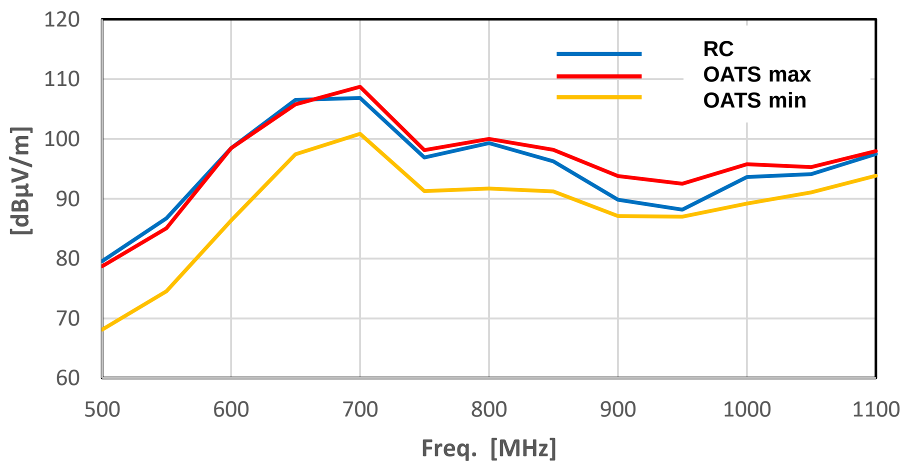

Good correlation with OATS

Immunity tests

$$E_{\mathrm{Eut}} = \left\langle \frac{8\pi}{\lambda}\sqrt{5\frac{P_{\mathrm{MaxRec}}}{\eta_{\mathrm{rx}}}} \right\rangle_n$$

$$\langle |E_x|_{\max} \rangle \approx \sqrt{\frac{\lambda \eta_V Q}{6\pi V}\left[0{,}577\,2 + \ln(N+1) - \frac{1}{2(N+1)}\right]\langle P_{\mathrm{Tx}} \rangle}$$

The maximum E field is of interest for the EUT malfunctioning

$$P_{input} = \left[\frac{E_{test}}{\langle E \rangle_{24 or 9}\sqrt{CLF(f)}}\right]^2$$

CLF ≤ 1

Accounts for quality factor variations w.r.t. calibration

Monitor and record:

- $P_{\text{rec. Max}}$ to estimate the maximum field
- $P_{\text{rec.Avg}}$ to control the loading (variations greater than 3 dB must be solved)

During calibration: P_{in} = 10 mW, Q = 5000, $\langle E_i \rangle$ = 3.5 V/m
For testing at 150 V/m: P_{in} = 18 W assuming CLF = 1
In anechoic chamber P_{in} ≈ 700 W (assuming G= 10 dB and r=3 m)

Example: coupling to a transmission line

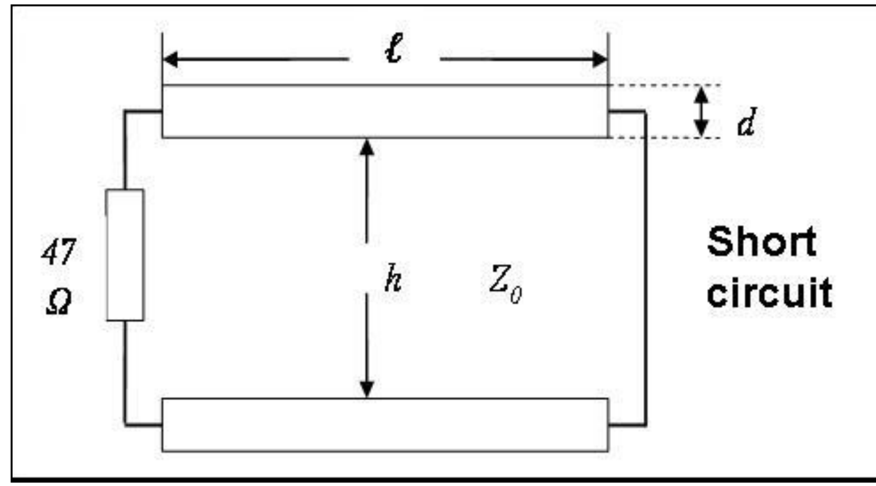

ℓ = 50 cm

h = 2.5 cm

Zo = 470 Ω

Results: effect of positioning and orientation

$\langle |I| \rangle_M$

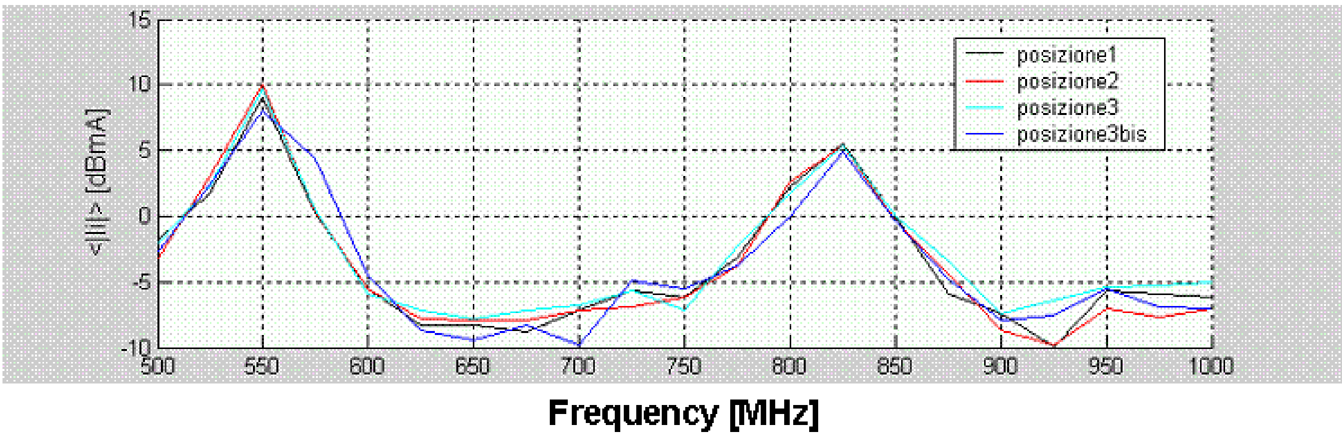

$|I| \uparrow_M$

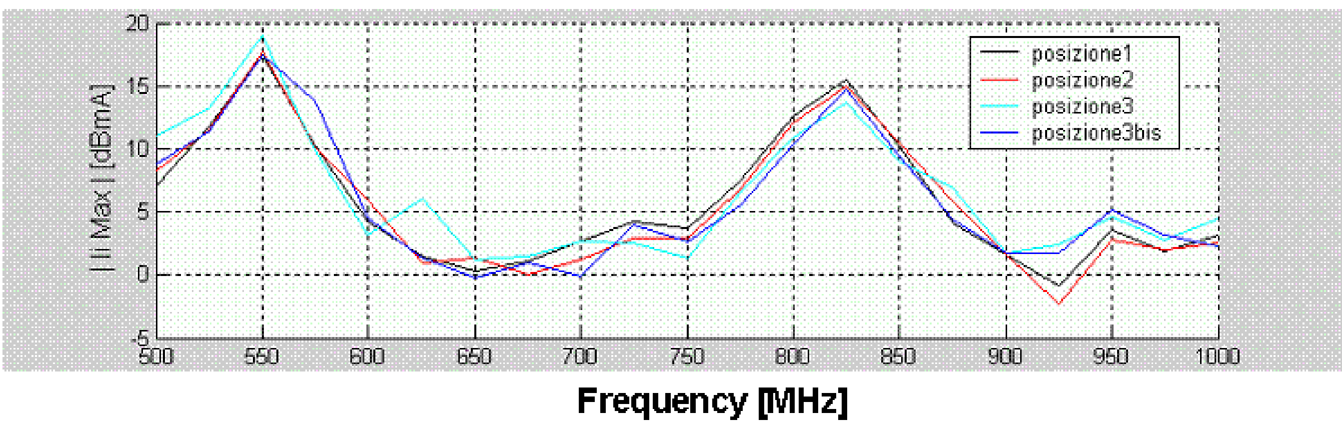

Maximum induced current

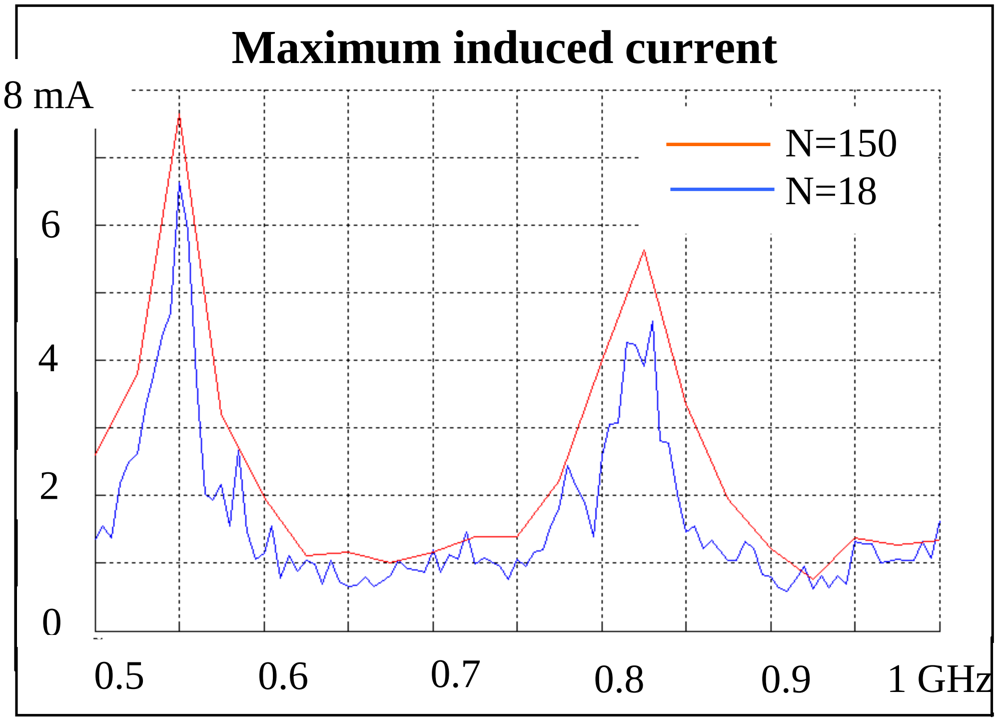

Max/mean ~ Ln (N) + 1/2N + 0,577

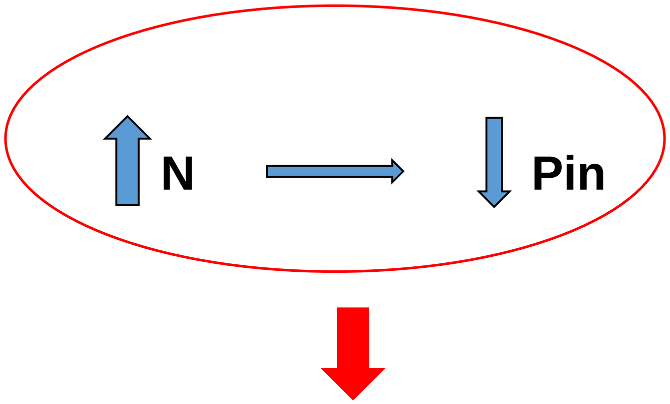

Increasing testing time

Pay attention when you operate in “stirring” w.r.t “tuned” mode

- All independent stirrer positions are employed
- Total stirrer independent positions depend on Q factor

Shielding effectiveness

Conventional methods often uses normal incidence plane wave (e.g. coaxial TEM fixture)

In real complex environments material are exposed to fields that impinge on the material with various polarizations and angle of incidence.

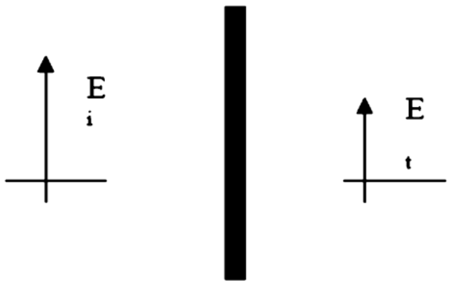

$$SE = -10Log_{10}\left(\frac{P_t}{P_i}\right)$$

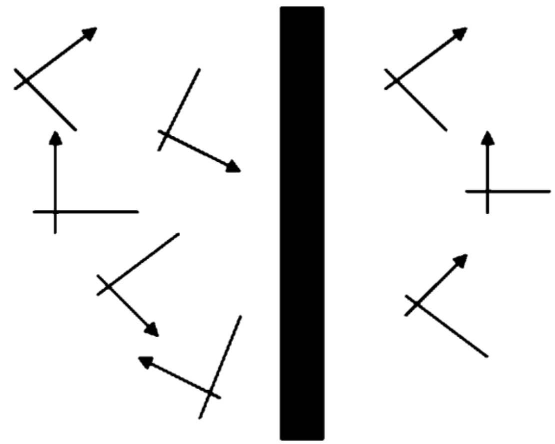

RC field excitation might be more representative of real life situations

Nested reverberation chamber for shielding effectiveness measurements

- The outer chamber provides a statistically random excitation of the sample under test
- The inner chamber provides a statistically uniform and isotropic field level due to the energy crossing the sample under test

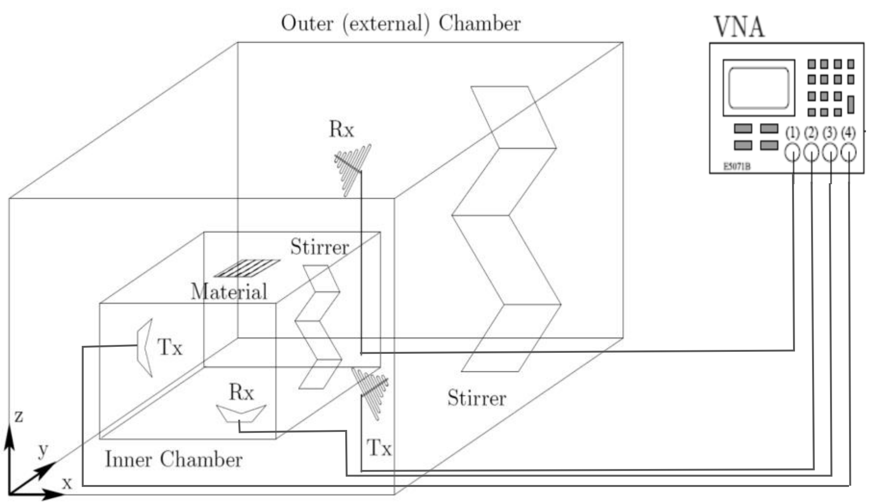

$$Q_{\mathrm{in},ns} = \frac{16\pi^2 V}{\lambda^3} \frac{P_{rQ,\mathrm{in},ns}}{P_{tx,\mathrm{in},ns}}$$

Sample insertion effect

$$Q_{\mathrm{in},s} = \frac{16\pi^2 V}{\lambda^3} \frac{P_{rQ,\mathrm{in},s}}{P_{tx,\mathrm{in},s}}$$

$$\mathrm{SE} = -10\log_{10}\left(\frac{P_{r,\mathrm{in},s}}{P_{r,\mathrm{in},ns}} \frac{P_{r,o,ns}}{P_{r,o,s}} \frac{P_{rQ,\mathrm{in},ns}}{P_{rQ,\mathrm{in},s}} \frac{P_{tx,\mathrm{in},s}}{P_{tx,\mathrm{in},ns}}\right)$$

SE of cementitious composites

Pristine MWCNTs
(Nanocyl™ NC 7000,
av. diameter ~ 9.5 nm,
av. length ~ 1.5 μm,
carbon purity ~ 90%,
surface area 250÷300 m^2/g)

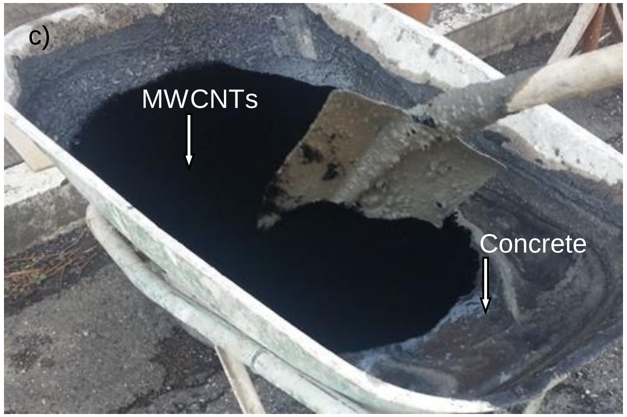

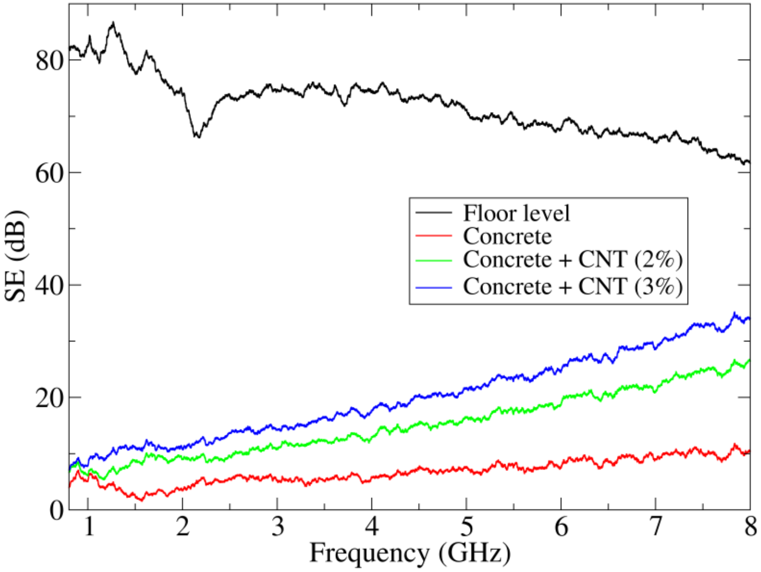

Averaged absorbing cross section (ACS)

$$ACS = \langle \sigma_{abs} \rangle = \frac{\langle P_{abs} \rangle}{S} \qquad Q_s = \frac{2\pi V}{\lambda \langle \sigma_a \rangle_\Omega} \qquad Q_s^{-1} = Q_l^{-1} - Q_u^{-1}$$

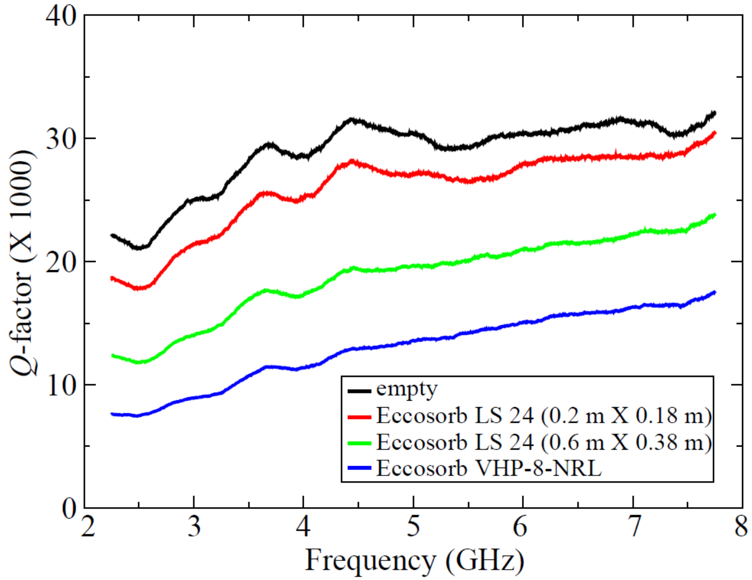

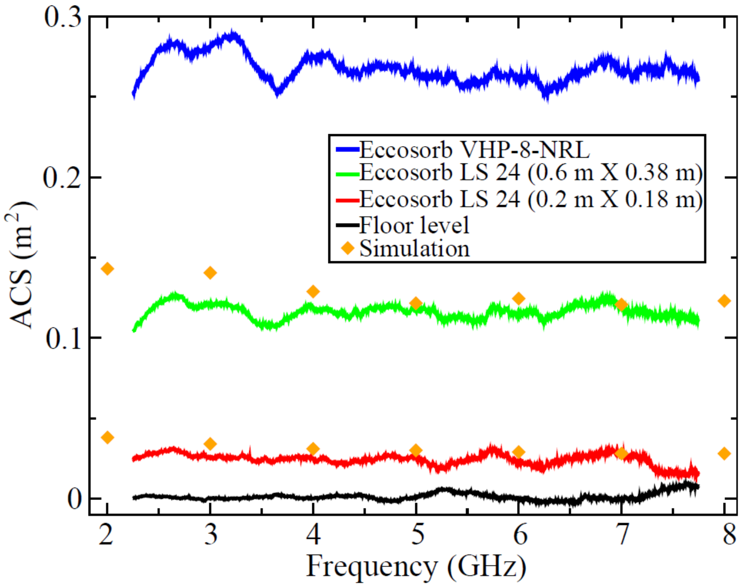

G. Gradoni, D. Micheli, F. Moglie, and V. Mariani Primiani, "Absorbing cross section in reverberation chamber: experimental and numerical results," *Progress In Electromagnetics Research B*, Vol. 45, 187-202, 2012.

Eccosorb VHP-8-NRL

Eccosorb LS-24L

High sensitivity to the insertion of small samples

Testing of wireless devices and systems

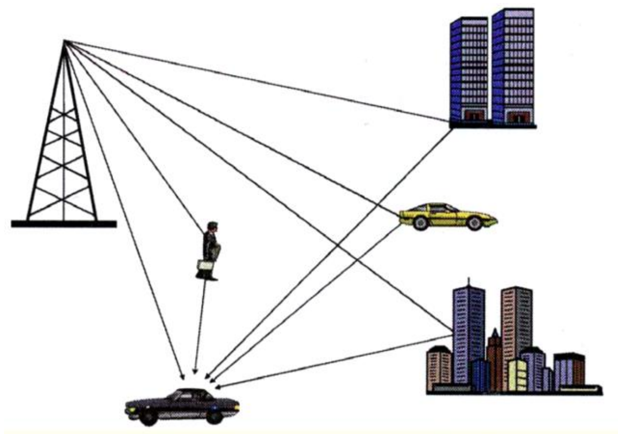

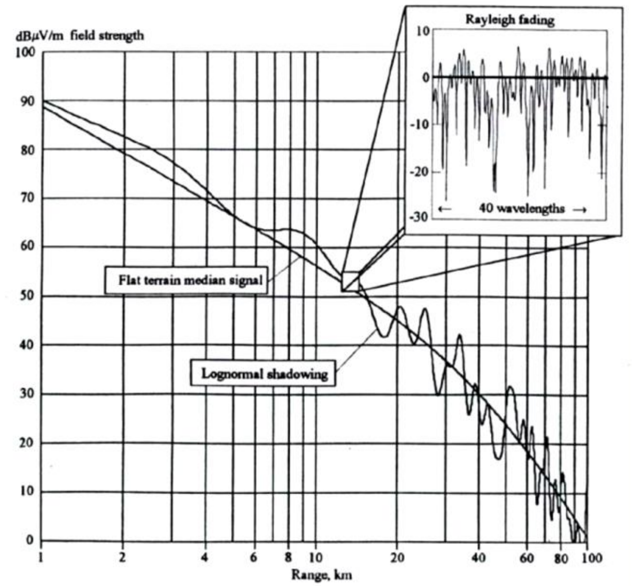

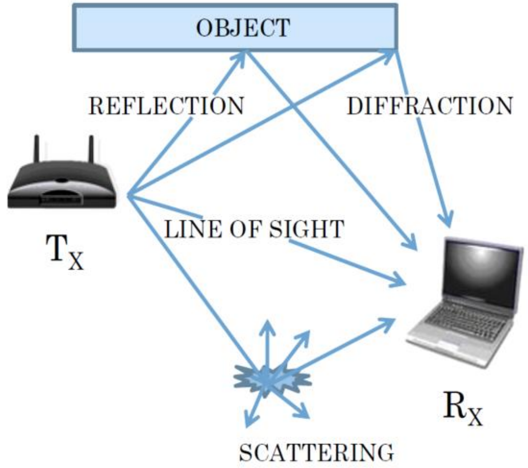

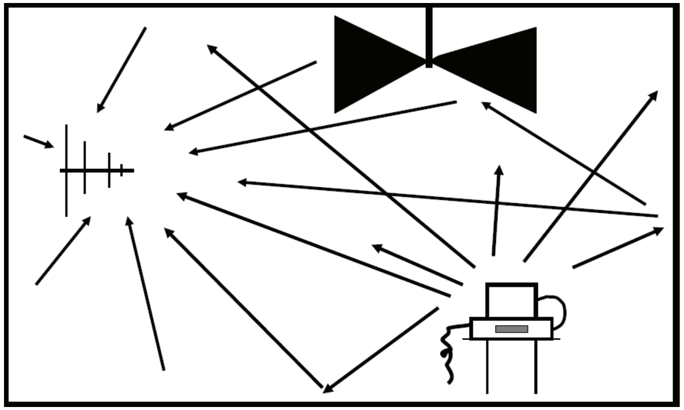

We have to move to a non-ideal RC

Distribuzione di Rayleigh

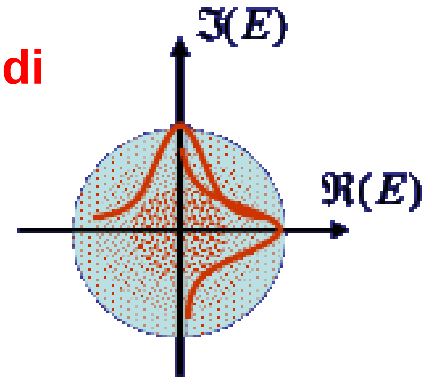

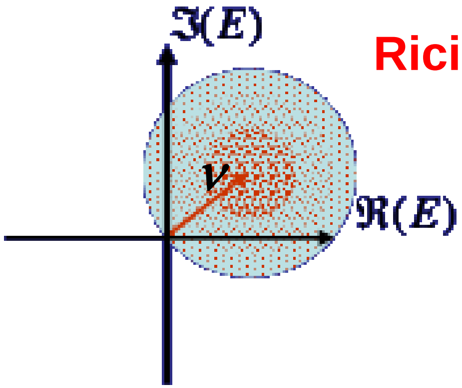

Rician distribution

$$f(E_x) = \frac{E_x}{\sigma_x^{\,2}} \cdot e^{-\frac{E_x^{\,2}}{2\sigma_x^{\,2}}}$$

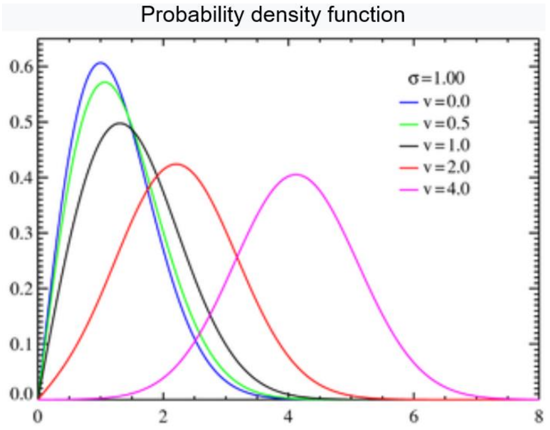

$$K = \frac{\nu^2}{2\sigma^2}$$

$$f(x \mid \nu, \sigma) = \frac{x}{\sigma^2} \exp\left(\frac{-(x^2+\nu^2)}{2\sigma^2}\right) I_0\left(\frac{x\nu}{\sigma^2}\right)$$

Testing of wireless devices and systems

ITU Report M.2135-1, Dec. 2009

Scenario		Delay spread (ns)
Indoor Hotspot	LOS	20
	NLOS	39
Urban Micro	LOS	65
	NLOS	129
	O-to-I	49
Suburban Macro	LOS	59
	NLOS	75
Urban Macro	LOS	93
	NLOS	365
Rural Macro	LOS	32
	NLOS	37

$$PDP(t) = \left\langle |h(t)|^2 \right\rangle_N \ , h(t) = \mathrm{IFT}[S_{21}]$$

$$\tau_{\mathrm{RMS}} = \frac{\sqrt{\int_0^\infty (t-\tau_{ave})^2 PDP(t)dt}}{\int_0^\infty PDP(t)dt}$$

$$\tau_{ave} = \frac{\int_0^\infty t\mathrm{PDP}(t)dt}{\int_0^\infty \mathrm{PDP}(t)dt}$$

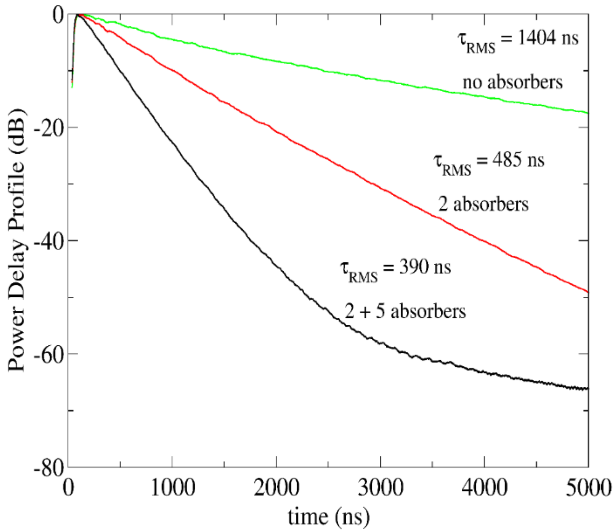

D. Micheli, M. Barazzetta, F. Moglie and V. Mariani Primiani, "Power Boosting and Compensation During OTA Testing of a Real 4G LTE Base Station in Reverberation Chamber," in *IEEE Transactions on Electromagnetic Compatibility*, vol. 57, no. 4, pp. 623-634, Aug. 2015.

Example of a transmission quality test

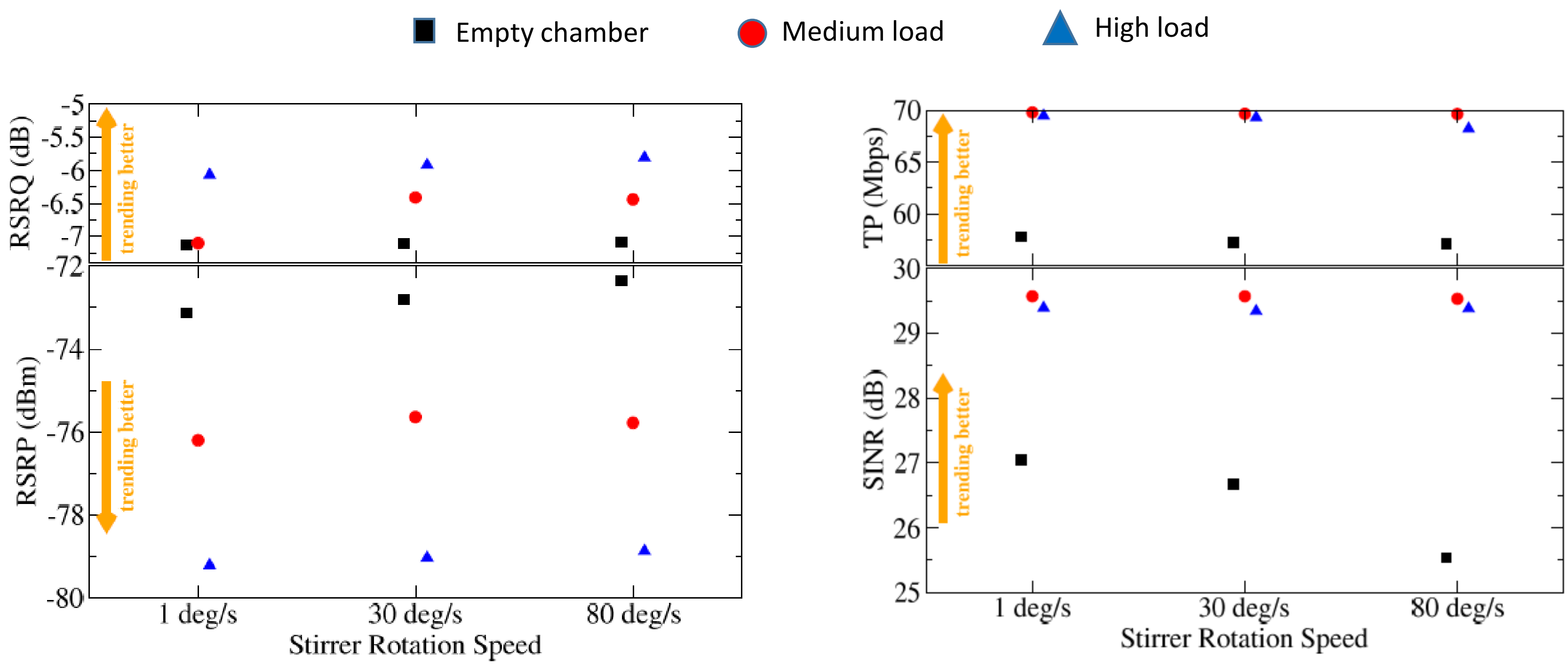

➢*Reference signal received power (RSRP): is the average* of the power of resource elements that carry cell-specific reference signals

➢*Reference signal received quality (RSRQ): is based on the ratio of* RSRP and RSSI (total wideband received power)

➢*PDSCH net throughput: is the throughput measured at* physical layer at the client in the data downlink channel, removing the re-transmissions of negatively acknowledged TBs.

➢*Signal to interference and noise ratio (SINR): is the ratio* between the wanted part of the signal and the sum of interference and noise

References

- IEC 61000-4-21, “Electromagnetic compatibility (EMC) - Part 4-21: Testing and measurement techniques – Reverberation chamber test methods”.
- David A. Hill, “Electromagnetic Fields in Cavities:Deterministic and Statistical Theories”, 2009, Wiley-IEEE Press
- Philippe Besnier, Bernard Démoulin, “Electromagnetic Reverberation Chambers”, Sep 2011, Wiley-ISTE.
- Stephen J. BoyesYi Huang, “Reverberation Chambers: Theory and Applications to EMC and Antenna Measurements”, 2015, John Wiley & Sons, Ltd.
- J. Ladbury, G. Koepke and D. Camell, “Evaluation of the NASA Langley Research Center Mode-Stirred Chamber Facility” NIST Technical Note 1508, January 1999
- R. Serra, A. Marvin, F. Leferink, V. Mariani Primiani, F. Moglie, M. O. Hatfield, Y. Huang. L. Arnaut, A. Cozza. M. Klinger, "Reverberation chambers a la carte: An overview of the different mode-stirring techniques," in *IEEE Electromagnetic Compatibility Magazine*, vol. 6, no. 1, pp. 63-78, First Quarter 2017.
- Arnaut, L R, “Measurement uncertainty for reverberation chambers - I. Sample statistics.”, NPL Report TQE 2, December 2008, ISSN: 1754-2995
- F. Leferink, “High Field Strength in a Large Volume: The Intrinsic Reverberation Chamber”, IEEE EMC 1998, Denver, CO, USA
- L. Arnaut, “Operation of electromagnetic reverberation chambers with wave diffractors at relatively low frequencies”, IEEE Trans. on EMC 2001, pp. 637-653, Vol. 43, No. 4, Nov.
- A. C. Marvin, E. Karadimou, ”The Use of Wave Diffusers to Reduce the Contribution of Specular Wall Reflections to the Unstirred Energy in a Reverberation Chamber”, IEEE EMC 2013, Denver, CO, USA

References, cont.

- F. Moglie and V. Mariani Primiani, "Numerical Analysis of a New Location for the Working Volume Inside a Reverberation Chamber," in *IEEE Transactions on Electromagnetic Compatibility*, vol. 54, no. 2, pp. 238-245, April 2012.
- C.L. Holloway, D.A. Hill, J. Ladbury, G. Koepke and R. Garzia, “Shielding Effectiveness Measurements of Materials Using Nested Reverberation Chambers,” in IEEE Trans. On Electromagnetic Compatibility, vol. 45, pp. 350-356, May 2003.
- D. Micheli, M. Barazzetta, F. Moglie and V. Mariani Primiani, "Power Boosting and Compensation During OTA Testing of a Real 4G LTE Base Station in Reverberation Chamber," in *IEEE Transactions on Electromagnetic Compatibility*, vol. 57, no. 4, pp. 623-634, Aug. 2015.
- K. Selemani, J.-B. Gros, E. Richalot, O. Legrand, O. Picon and F. Mortessagne, “Comparison of reverberation chamber shapes inspired from chaotic cavities”, IEEE Trans. on EMC 2015, pp. 3-11, Vol. 57, No. 1, Feb

Many, many others .. sorry for missing.

Dedicated sessions at Conferences

- EMC Europe 2018, INTERNATIONAL SYMPOSIUM AND EXHIBITION ON ELECTROMAGNETIC COMPATIBILITY, 27-30 AUG., AMSTERDAM.
- IEEE EMCS Symposium on ELECTROMAGNETIC COMPATIBILITY, SIGNAL & POWER INTEGRITY, July 30 - August 3, 2018, Long Beach (CA).